Magnetohydrodynamics simulation of plasma processes in a helicon plasma source for a MW-level electromagnetic thruster at LIP

IEPC-2017-77

Presented at the 35th International Electric Propulsion Conference
Georgia Institute of Technology • Atlanta, Georgia • USA
October 8 – 12, 2017

Xiaodong Wen[1], Tianping Zhang[2], Yanhui Jia[3], Chenchen Wu[4], Ning Guo[5] and Xinfeng Sun[6]
Lanzhou Institute of Physics, Lanzhou City, Gansu Province, 730000, China

Abstract: A Megawatt-level electromagnetic thruster with a helicon plasma source and a RMF acceleration section is under developing at Lanzhou Institute of Physics (LIP). In the first stage, a 5 kW downscaled thruster prototype whose helicon discharge power is 1 kW is designing now for acceleration principle demonstration. This paper presents the design and optimization of the helicon plasma source by calculating the plasma resistance using HELIC code with different helicon antenna lengths and axial magnetic fields both considering classical helicon wave and Trivelpiece-Gould (TG) mode. With the optimized helicon plasma source, a 3D helicon discharge model is established by COMSOL Multiphysics™ Software hence the dynamic plasma processes in the optimized helicon plasma source are detailed simulated. The simulation results show that with an optimized Nagoya III type helicon antenna, a plasma density nearly up to 3×10^{19} m^{-3} using the Argon gas is achieved under the RF power up to 1kW driven at 13.56MHz.

Nomenclature

$\boldsymbol{B}$	=	magnetic flux density vector
$\boldsymbol{D}_e$	=	electron diffusion coefficient
$\boldsymbol{D}_\varepsilon$	=	electron energy diffusion coefficient
$\boldsymbol{E}$	=	electric field vector
$\boldsymbol{H}$	=	magnetic field strength vector
L_a	=	helicon antenna length
n_e	=	plasma density
n_ε	=	electron energy density
Q_{abs}	=	absorbed RF power by plasma
R	=	plasma resistance
ω	=	angular frequency of RF current
$\boldsymbol{\mu}_e$	=	electron mobility
$\boldsymbol{\mu}_\varepsilon$	=	electron energy mobility
Γ_e	=	electron flux
Γ_ε	=	electron energy flux

[1] Engineer, Science and Technology on Vacuum Technology and Physics Laboratory, wenxd06@gmail.com.
[2] Professor, Science and Technology on Vacuum Technology and Physics Laboratory, ztp510@aliyun.com.
[3] Senior Engineer, Science and Technology on Vacuum Technology and Physics Laboratory, jiayh510@163.com.
[4] Engineer, Science and Technology on Vacuum Technology and Physics Laboratory, wuchenchen2008kaka@163.com.
[5] Professor, Science and Technology on Vacuum Technology and Physics Laboratory, guoningaa@163.com.
[6] Engineer, Science and Technology on Vacuum Technology and Physics Laboratory, xinfenghappy@126.com.

I.Introduction

The rapid increasing of space missions like deep space exploration, Mars landing and orbit transfer, imposes a urgent requirement for high power electric propulsion due to its high specific impulse which cannot be realized by traditional chemical propulsion. In past decades, several high power electric thrusters such as MPDT[1], PIT[2], NHT[3], VASIMR[4] and ELF[5] have been studied and developed extensively. Among them, ELF thrusters developed by University of Washington and MSNW LCC show great potentials to operate up to MW power levels with extremely long operation lifetime due to its high energy density, electrodeless design, lightweight and compaction. Based on the pulsed creation, confinement and acceleration of a high-density, magnetized Field Reversed Configuration (FRC) plasmoid by employing a Rotating Magnetic Field (RMF), ELF thrusters can perform steadily over a very wide range of input power while keeping relatively high efficiencies. Besides ELF thrusters, a Helicon Electrodeless Advanced Thruster (HEAT)[6] and a Gradually Expanded Rotamak-like (GER)[7] plasma thruster are also proposed respectively in Japan and Singapore which are both based on the FRC plasmoid generated by RMF.

In past years, a megawatt-level electromagnetic thruster with a helicon plasma source and a tapered RMF acceleration section has been proposed by Lanzhou Institute of Physics (LIP). Recently, we are designing a 5 kW downscaled thruster prototype to demonstrate the plasma generation, confinement and acceleration. As the first step, the helicon plasma source must be designed and optimized carefully to meet the requirements of RMF acceleration scheme. For plasma discharges, direct 3D simulation for different parameter scanning is quite inefficiency even by MHD method due to its complicated since the involving of magnetic fields, plasma chemical reaction and anomalous antenna. Fortunately, the HELIC code[8] written by Donald Arnush provide a simple but efficiency tool to design and optimize the basic parameters such as the diameters and lengths of helicon plasma source very quickly. With the optimized helicon plasma source, a 3D model is then constructed by COMSOL Multiphysics™ software and the dynamic plasma processes is simulated using magnetohydrodynamics (MHD) method. The simulation results give detailed descriptions of the RF power coupling and absorption, plasma resistance and antenna excitation.

The outline of this paper is as follows: The basic parameter design and optimization of helicon plasma source is described in Sec. II. The calculated 3D model and the simulation results are given in Sec. III and Sec. IV, respectively. Finally, conclusion and discussion are presented in Sec. V.

II. Helicon Plasma Source Design

In present design, helicon waves with the azimuthal mode m=1 will be excited in Argon gas by a Nagoya III helicon antenna driven at 13.56 MHz. Based on the preliminary studies and present engineering considerations, the outer diameter and axial length of the helicon plasma source chamber are determined to be 23 mm and 100 mm, respectively. Thus the length of the helicon antenna and the external axial magnetic field are the two critical parameters for helicon plasma source design and optimization which is calculated numerically by HELIC code. In the calculation, the plasma density and the magnetic field strength are respectively assumed in a range of 1×10^{12} - 5×10^{13} cm^{-3} and 50 - 500 Gs. The radial distribution of plasma density is nonuniform with a profile as shown in Figure 1 along with a plasma radius of 20 mm. The antenna is located at the end of the discharge chamber with an insulating boundary condition at the both ends. The neutral pressure of Argon gas and the electron temperature used in the collision factor are 75 mTorr and 3 eV, respectively.

One of the most important parameters is the plasma resistance R which is proportional to the RF energy absorption. This quantity should be larger than 1 Ω to eliminate circuit resistance loss thus to keep the RF power depositing mostly in the plasma itself rather than in the circuitry[9]. The calculated plasma resistances R with different helicon antenna lengths versus plasma density n_e and external axial magnetic field strength B are shown in Figure 2. The results show that with an antenna length of 100 mm and an axial magnetic field strength of 500 Gs, the plasma resistance can be larger than 2 Ω (maximal 2.4 Ω) while the plasma density larger than 7×10^{12} cm^{-3} at a stable operation which occurs on the downward slop of each peak. This plasma density is high enough for the following RMF acceleration.

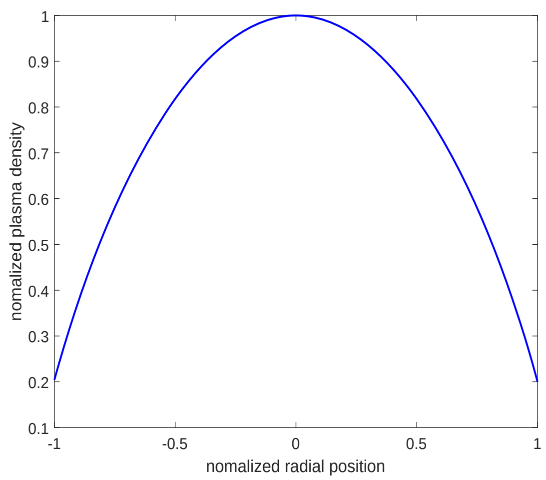

Figure 1. Assumed plasma density radial distribution.

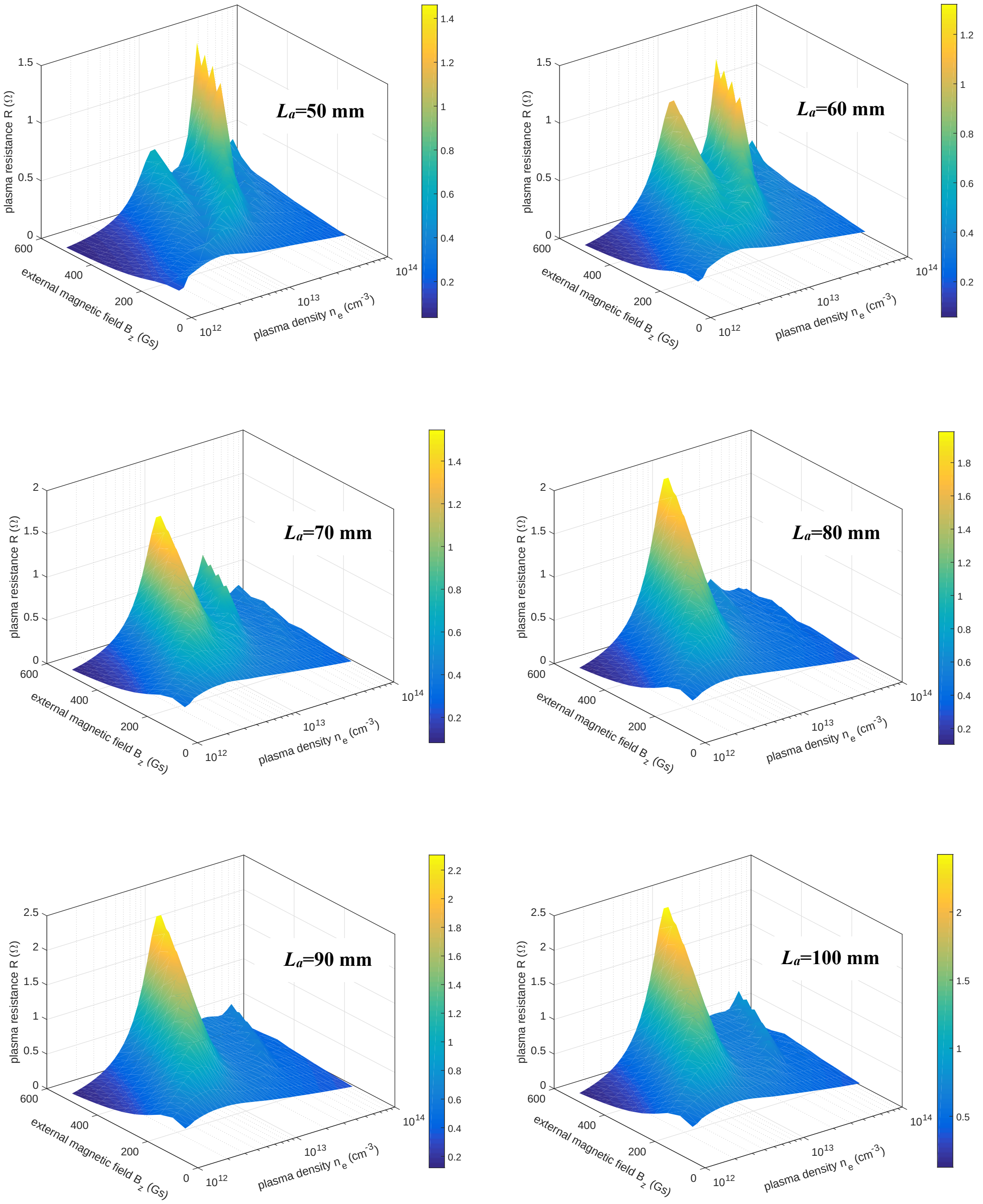

Figure 2. Calculated plasma resistance *R* vs. n_e and *B* for different antenna length obtained by HELIC

III. 3D Simulation Model Setup

A. Model Description

The 3D simulation model established by COMSOL Multiphysics™ Software is shown in Figure 3. A Nagoya III type helicon antenna driven at 13.56 MHz with a length of 100 mm is applied to excite helicon waves whose azimuthal mode number is 1 in a axial symmetrical plasma column. The background axial magnetic field and gas pressure are both uniformly distributed with values of 500 Gs and 75 mTorr.

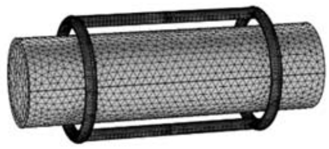

Figure 3. Helicon plasma discharge model

B. Equations for Fluid Plasma Model

For the helicon plasma discharge, the momentum transfer collisional frequency is larger than the radio frequency (RF) driving frequency which is 13.56 MHz here. Thus the general flux balance equation for electrons can be instead by drift-diffusion (DD) approximation[10] which can be expressed as:

$$\frac{\partial n_e}{\partial t} + \nabla \cdot \Gamma_e = S_e \tag{1}$$

where S_e is the source terms for electrons. The electron flux Γ_e is defined as:

$$\Gamma_e = -n_e(\boldsymbol{\mu}_e \cdot \boldsymbol{E}) - \boldsymbol{D}_e \cdot \nabla n_e \tag{2}$$

where $\boldsymbol{E}$ is the electric field strength which causes electrons movement with an electron mobility $\boldsymbol{\mu}_e$, $\boldsymbol{D}_e$ is electron diffusion coefficient which causes electrons diffusion. Assuming that the electrons have a Maxwellian distribution in the velocity phase space, the mobility here which is a tensor when a magnetic field is applied satisfy:

$$\mu_e^{-1} = \mu_{e0}^{-1}\begin{pmatrix} 1 & -\mu_{e0}B_z & 0 \\ \mu_{e0}B_z & 1 & 0 \\ 0 & 0 & 1 \end{pmatrix} \tag{3}$$

here μ_{e0} is the scalar electron mobility in the absence of the applied magnetic field and B_z is the axial component of the magnetic field vector.

The electron mean energy density conservation equation can also be expressed as:

$$\frac{\partial n_\varepsilon}{\partial t} + \nabla \cdot \boldsymbol{\Gamma}_\varepsilon + \boldsymbol{E} \cdot \boldsymbol{\Gamma}_\varepsilon = S_\varepsilon + Q_{abs}/e \tag{4}$$

the electron energy change caused by electric field $\boldsymbol{E}$ and inelastic collisions are respectively denoted by $\boldsymbol{E} \cdot \boldsymbol{\Gamma}_\varepsilon$ and S_ε, while Q_{abs} is the energy coupled RF power into the plasma column. Similar to the definition of the electron flux Γ_e, the electron energy flux density is defined as:

$$\boldsymbol{\Gamma}_\varepsilon = -n_\varepsilon(\boldsymbol{\mu}_\varepsilon \cdot \boldsymbol{E}) - \boldsymbol{D}_\varepsilon \cdot \nabla n_\varepsilon \tag{5}$$

here $\boldsymbol{D}_\varepsilon$ and $\boldsymbol{\mu}_\varepsilon$ are electron energy diffusion coefficient and mobility which are related to $\boldsymbol{D}_e$ and $\boldsymbol{\mu}_e$ by[11]

$$\begin{aligned} \boldsymbol{\mu}_\varepsilon &= 5\boldsymbol{\mu}_e/3 \\ \boldsymbol{D}_\varepsilon &= 5\boldsymbol{D}_e/3 \end{aligned} \tag{6}$$

when the electron energy distribution function (EEDF) is Maxwellian.

As the skin depth of RF current driven at 13.56 MHz is only 18 μm in the copper antenna, the computation will be quite huge and slow with proper meshing. Fortunately, an impedance boundary condition can be introduced to dramatically reduce the computation. In this boundary condition, the electromagnetic field induced by a current source can be written as:

$$\sqrt{\frac{\mu_0\mu_r}{\varepsilon_0\varepsilon_r - j\sigma/\omega}} \cdot \boldsymbol{n} \times \boldsymbol{H} + \boldsymbol{E} - (\boldsymbol{n} \cdot \boldsymbol{E})\boldsymbol{n} = 0 \tag{7}$$

where μ_r, ε_r and σ are respectively relative permeability, relative dielectric constant and conductivity of the helicon antenna, ω is the angular frequency of RF current.

C. Plasma Chemical Reaction

During the helicon plasma discharge processes for Argon gas, there are seven particle collision reactions and two surface reactions are under consideration as listed in Table 1. The collision corss-section[12] of some major reactions are shown in Figure 4.

Table 1. Table of collisions and reactions modeled

Reaction	Formula	Type	Δε (eV)
1	e+Ar=e+Ar	elastic	0
2	e+Ar=e+Ars	excitation	11.5
3	e+Ars=e+Ar	superelastic	-11.5
4	$e+Ar=2e+Ar^+$	ionization	15.8
5	$e+Ars=2e+Ar^+$	ionization	4.24
6	$Ars+Ars=e+Ar+Ar^+$	Penning ionization	-
7	Ars+Ar=Ar+Ar	metastable quenching	-
8	Ars=Ar	deexcitation	-
9	$e+Ar^+=Ar$	recombination	-

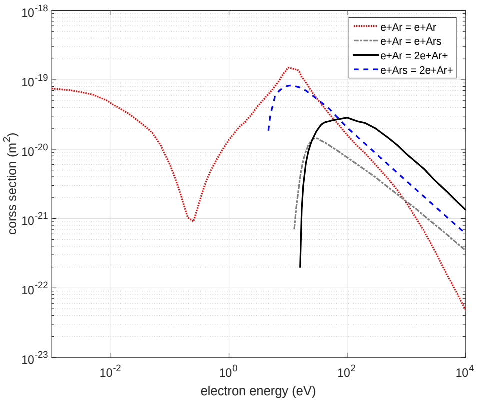

Figure 4. Collision cross sections for Argon

IV. Simulation Results

The simulated electron density distributions in two cross sections are shown in Figure 5, while the axial and radial distributions are depicted in Figure 6.

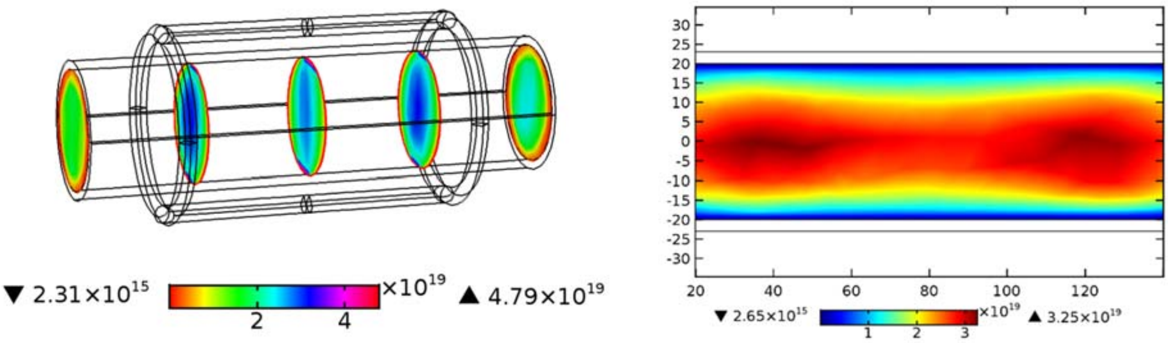

Figure 5. electron density distributions in transverse cross section (left) and in side view (right)

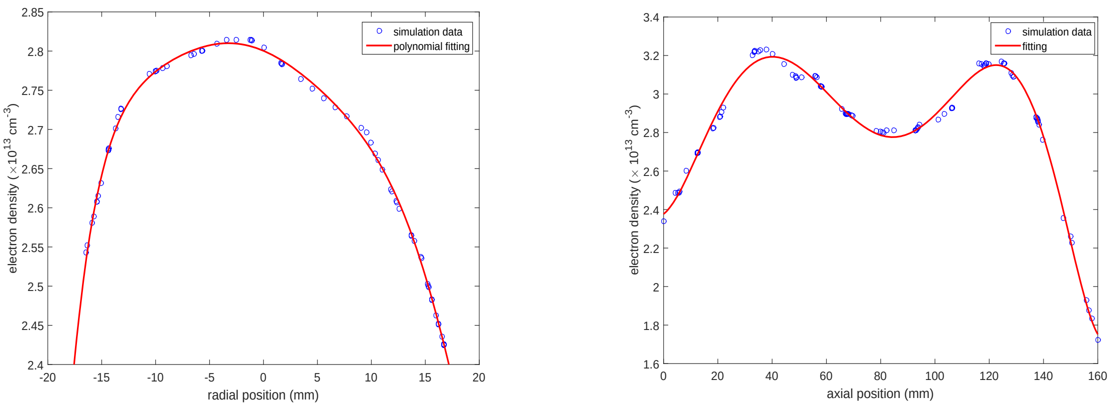

Figure 6. Radial (left) and axial (right) distributions of the electron density

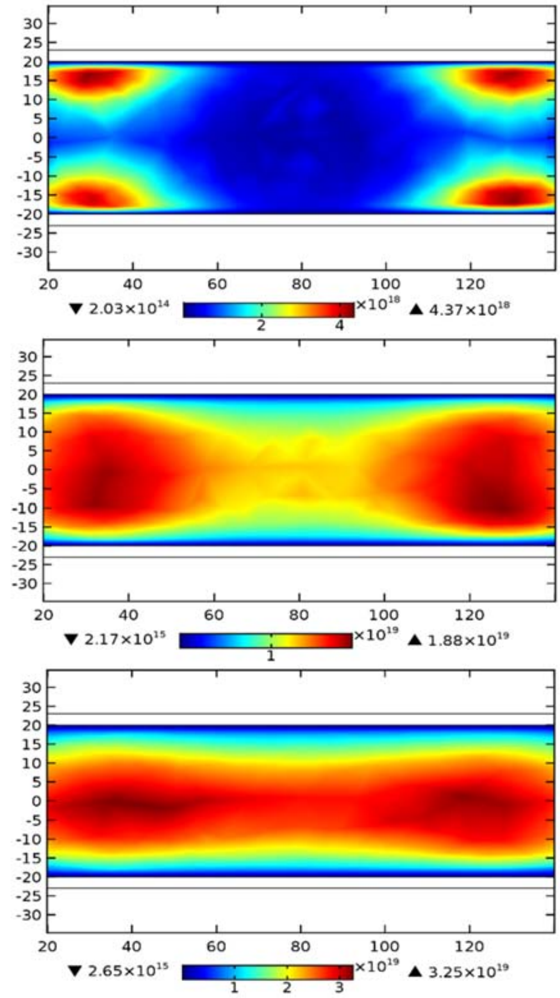

Figure 7. Electron density evolution at time of 1 μs (top), 23 μs (middle) and 1.3 ms (bottom)

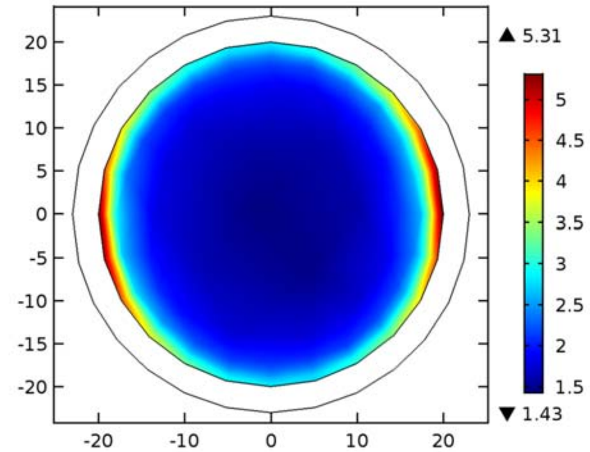

Figure 8. Electron temperature in eV at time of 10 ms

From the figures in the left, the maximal electron density in the plasma column is about 3.23×10^{19} m^{-3} which occurs at the position of the two circle legs of the helicon antenna. Meanwhile, in most of the plasma column, the electron density is nearly 2.7×10^{19} m^{-3} which is a relatively high density for the following RMF acceleration. In the transverse cross section, the electron density has a peak in the center. The electron density evolutions along the radial position at different time are shown in Figure 7.

As shown in Figure 7, the helicon discharge starts at regions close to the circle legs of the Nagoya III helicon antenna and gradually expand to the center of the discharge chamber. By tracking the evolution process, on found that the discharge achieve stability at the time about 1 ms and the electron density does not change any more. Meanwhile, the electron density gradually increases both in radial and axial directions before the discharge stability.

The cross section distribution of electron temperature in eV at the chamber center is illustrated in Figure 8. As shown in this figure, except the edge region, the electron temperature in the plasma column is less than 2.5 eV which is relatively not very high. With a strong magnetic field (500 Gs), the electrons are magnetized and have cyclotron gyration which make themselves collide with neutral atoms much easier in the discharge chamber. Consequently, electrons lose their energy by the collisions so frequently that they cannot accumulate enough energy to achieve high plasma temperature.

V. Conclusion

A 1 kW helicon plasma source driven at 13.56 MHz with a Nagoya III antenna has been designed and optimized by numerical solutions. By calculating the plasma resistance which actually is a reflection of RF power coupling to the plasma, the length of the helicon antenna and the external axial magnetic field strength are respectively determined to be 100 mm and 500 Gs with a plasma resistance uo to 2.4 Ω. To study the dynamic discharge processes of helicon wave excitation detailedly, we established a full three-dimensional model based on magnetohydrodynamics method by using COMSOL Multiphysics^{TM} Software. The simulation results show that the discharge remains unchanged after about 1 ms. The helicon discharge for Nagoya III antenna start at the region close to its two the circle legs and then gradually expands to the whole plasma column. At the stable plasma state, the maximal plasma density is up to 3.23×10^{19} m^{-3} and remains nearly 2.7×10^{19} m^{-3} in most regions of the chamber. As the electrons are confined by a relatively strong magnetic field, the electron temperature (energy) is approximately less than 2 eV due to their frequent collisions with neutral atoms which lead to a high density plasma. The helicon plasma source will be further optimized to meet the requirements of RMF acceleration for the whole prototype thruster.

Acknowledgments

The authors thank Professor Francis F. Chen and Dr. Donald Arnush for offering the HELIC code for free and some profitable suggestions in using this code. The authors also thank Dr. Haili Wang for optimizing the COMSOL Multiphysics model.

References

[1] Yuya Oshio, Satoshi Tonooka, Ikkoh Funaki, "Thrust Performance and Cathode Temperature Evaluation of MW Class Quasi-Steady MPD Thruster," *Proceedings of the 52nd AIAA/SAE/ASEE Joint Propulsion Conference*, AIAA 2016-5039, Salt Lake City, 2016, pp. 1-11.

[2] Ashley K. Hallock, Adam K. Martin, Kurt A. Polzin, Adam C. Kimberlin, and Richard H. Eskridge, "Single- and Repetitive-Pulse Conical Theta-Pinch Inductive Pulsed Plasma Thruster Performance", *IEEE Transactions on Plasma Science*, Vol. 43, No. 1, 2015, pp. 433-443.

[3] Scott J. Hall, Sarah E. Cusson, Alec D. Gallimorez, "30-kW Performance of a 100-kW Class Nested-channel Hall Thruster", *Proceedings of the 34th International Electric Propulsion Conference*, IEPC-2015-125, Hyogo-Kobe, Japan, 2015, pp. 1-15.

[4] Jared P. Squire, Mark D. Carter, Franklin R. Chang Díaz, Lawrence Dean, Matthew Giambusso, Tim G. Glover, Jose Castro, and Juan Del Valle, "Advances in Duration Testing of the VASIMR® VX-200SS System", *Proceedings of the 52nd AIAA/SAE/ASEE Joint Propulsion Conference*, AIAA 2016-4950, Salt Lake City, 2016, pp. 1-10.

[5] Anthony P. Pancotti, Justin M. Little, Jordan S. Neuhoff, Barry M. Cornella, David E. Kirtley, and John T. Slough, "Electrodeless Lorentz Force (ELF) Thruster for ISRU and Sample Return Mission", *Proceedings of the 34th International Electric Propulsion Conference*, IEPC-2015-67, Hyogo-Kobe, Japan, 2015, pp. 1-10.

[6] T. Furukawa, K. Takizaka, D. Kuwahara, and S. Shinohara, "Study on Electromagnetic Plasma Propulsion using Rotating Magnetic Filed Acceleration Scheme", *Physics of Plasma*, Vol. 24, No. 4, 2017, pp. 043505.

[7] Shuyan Xu, "GER: Gradually Expanded Rotamak-like Plasma Thruster", *Presentation of the 3rd Singapore Space Symposium*, Sigapore, 2016.

[8] Donald Arnush, "The Role of Trivelpiece–Gould Waves in Antenna Coupling to Helicon Waves", *Physics of Plasma*, Vol. 7, No. 7, 2000, pp. 3042-3050.

[9] Francis F. Chen, "Ion Ejection from a Permanent-magnet Mini-helicon Thruster", *Physics of Plasma*, Vol. 21, No. 9, 2014, pp. 093511.

[10] H. C. Kim, F. Iza, S. S. Yang, M. Radmilović-Radjenović, and J. K. Lee, "Particle and Fluid Simulations of Low-temperature Plasma Discharges: Benchmarks and Kinetic Effects", *Journal of Physics D: Applied Physics*, Vol. 38, No. 19, 2005, pp. R283-R301.

[11] G. J. M. Hagelaar, and L. C. Pitchford, "Solving the Boltzmann Equation to Obtain Electron Transport Coefficients and Rate Coefficients for Fluid Models", *Plasma Source Science and Technology*, Vol. 14, No. 4, 2005, pp. 722-733.

[12] L. C. Pitchford, L. L. Alves, K. Bartschat, S. F. Biagi, M. C. Bordage, A. V. Phelps, C. M. Ferreira, G. J. M. Hagelaar, W. L. Morgan, S. Pancheshnyi, V. Puech, A. Stauffer, and O. Zatsarinny, "Comparisons of sets of electronCneutral scattering cross sections and swarm parameters in noble gases: I. Argon", *Journal of Physics D: Applied Physics*, Vol. 46, No. 33, 2013, pp. 1-19.